Journal of Optoelectronics and Advanced Materials, Vol. 4, No. 2, June 2002, p. 199 - 205

MAGNETIC PROPERTIES OF (Fe,Co)-(Al,Ga,Si)-(B,C,P) ALLOYS WITH LARGE SUPERCOOLED LIQUID REGION: INFLUENCE OF PREPARATION CONDITIONS AND HEAT TREATMENT

S. Roth, H. Grahl, J. Degmova, N. Schlorke-de Boer, M. Stoica, J.M. Borrego[a], A. Conde[a], N.M. Mitrovic[b], J.Eckert

IFW Dresden, Dresden, Germany
[a]University of Seville, Seville, Spain
[b]Technical Faculty Cacak, Cacak, Yugoslavia

Amorphous materials with a wide supercooled liquid region, which is defined by the difference between the glass transition temperature T_g and the crystallization temperature T_x, give promise to expand the application field of amorphous iron-base alloys as soft magnetic materials. It may be possible to cast such alloys directly for use as bulk components of magnetic cores or to make dense powder compacts by pressing at temperature between the glass transition temperature and the crystallization temperature. Melt spinning and centrifugal casting were used to prepare 3 to 10 mm wide and 20 to 50 μm thick amorphous ribbons, as well as rods with diameters of about 2 mm from Fe-TM-Al-P-B-C-Ga-Si-base alloys (TM = Nb, Co). Some of the ribbons were milled to powder, which was hot pressed to disks of 10 mm diameter and 2 to 6 mm height. The samples were characterized by X-ray diffraction (XRD), differential thermal calorimetry (DSC), thermogravimetry, (TMG), and the magnetic properties such as coercivity, H_c, saturation polarization, J_s, Curie temperature T_c, and magnetostriction constant, λ_s, were determined. The influence of preparation conditions, composition, and thermal treatment on the magnetic properties is discussed.

(Received February 21, 2002; accepted May 15, 2002)

Keywords: Iron-base alloys, Amorphous alloys, Soft magnetic materials, Magnetic properties

1. Introduction

Amorphous alloys are good candidates for soft magnetic materials because of the lack of crystal anisotropy. The only sources of unwanted anisotropies are the shape anisotropy due to surface roughness and the stress-induced anisotropy produced during the rapid quenching. This is the reason why amorphous soft magnetic materials became a well-defined class of materials [1]. Further improvements may be expected, if these unwanted anisotropies are reduced. Amorphous materials with a wide supercooled liquid region, which is defined by the difference between the glass transition temperature T_g and the crystallization temperature T_x, give an opportunity to achieve these: (i) the material may be cast into thicker ribbons due to the lower cooling rates necessary to obtain them in the amorphous state, and thus, the influence of the surface is reduced; (ii) the existence of a wide supercooled liquid region allows annealing at or above the glass transition temperature in the "liquid"-state and nearly complete stress relief may be expected; provided cooling from the annealing temperature is not inhomogeneous and causes no new internal stresses. Furthermore, it may be possible to cast such alloys directly and to use them as components of magnetic cores or to make dense powder compacts at a moderate pressing temperature between glass transition temperature and crystallization temperature.

2. Experimental

Multicomponent crystalline pre-alloys were prepared by arc melting under a Ti-gettered argon atmosphere using elements of high purity (metals: 99.99%, FeC and FeB: 99.5%, FeP: 97.5%). Ribbons were prepared by single roller melt spinning. Rods of 1 to 2 mm diameter were cast into a cold copper mold by centrifugal casting. Melt-spun ribbons were milled in a Retsch PM 4000 planetary mill under argon atmosphere for 30 min at 250 rpm. Powders were hot pressed at a pressure of 500 MPa for 2 min under argon atmosphere. Annealing was performed either in argon atmosphere by conventional furnace annealing (FA) or by joule (current) heating in air (CA). The amorphous character of the as-quenched samples and the crystallization products after annealing were examined by X-ray diffraction (XRD). The thermal stability of the supercooled liquid region, the glass transition temperature, T_g, and the onset crystallization temperature, T_x, were determined by differential scanning calorimetry (DSC) under argon atmosphere. The magnetization, M, in a field of 460 kA m^{-1} was measured as a function of temperature with a Faraday magnetometer which was also used to investigate the isothermal crystallization kinetics. The coercive field, H_c, and the saturation magnetostriction, λ_S, were measured at room temperature by a Förster Koerzimat and by the small-angle magnetization rotations method after Narita [2], respectively. The saturation polarization, J_s, at room temperature was measured with a vibrating sample magnetometer (VSM) using a maximum field of 1500 kA m^{-1} and at 10 K with a SQUID magnetometer using an applied magnetic field of 5 T. Quasistatic hysteresis loops were measured using a hysteresis loop tracer.

3. Results

3.1. Influence of composition

Amorphous Fe-Al-Ga-P-C-B-Si alloys are known to have interesting soft magnetic properties combined with a good glass-forming ability promising the formation of bulk soft magnetic materials. The replacement of iron by other transition metals may further improve these alloys. Therefore, amorphous ribbons of compositions $(Fe_xCo_yB_zC_u)_{80}Si_3Al_5Ga_2P_{10}$ (Table 1) were investigated. For temperatures between 650 and 900 K the differential scanning calorimetry (DSC) curves of all the as-quenched alloys show first an endothermic event due to the glass transition, followed by a distinct supercooled liquid region and then a sharp exothermic peak due to crystallization. A broad exothermic maximum due to structural relaxation can be observed for all the alloys prior to the glass transition. The thermal stability of the alloys does not show a monotonous dependence with Co content: T_x is not affected by Co substitution up to about 26 at. % and shows an increase of about 20 K for more than 52 at. % Co (Table 1). It should be noted that the changes in the B and C content (keeping the metalloid content constant) might affect this behavior too, although similar tendency was found in $Fe_{76.5}Co_xSi_{15.5}B_7Cu_1Nb_3$ alloys where B content was kept constant [3]. The glass transition temperature increases monotonously as Co increases (see Table 1). Therefore, the stability of glassy state, evaluated in terms of ΔT_x (= T_x -T_g), is not improved with the Co substitution.

Table 1. Glass transition temperature, T_g, on-set crystallization temperature, T_x, and Curie temperature, T_C, for $(Fe_xCo_yB_zCu_u)_{80}Si_3Al_5Ga_2P_{10}$ amorphous alloys.

x	70	56	43	29	17	5
y	0	14	26	40	52	63
z	5	6	8	9	10	12
u	5	4	3	2	1	0
T_g (K)	757	766	770	775	786	796
T_x (K)	815	815	815	823	836	836
T_C (K)	568	554	526	463	373	328

T_C decreases monotonously as the Co content increases. This dependence of T_C, similar to that found for $(Fe_{1-x}Co_x)_{62.5}Si_{12.5}B_{25}$ alloys [4], is different from that observed in amorphous Fe-Co-based alloys with lower metalloid concentration for which T_C shows a maximum for equiatomic Fe/Co compositions [5,6]. The strong descent of T_C with Co content can be mainly attributed to the decrease of the exchange interaction between Co-Co pairs provoked by the presence of the metalloid [4].

Fig. 1 shows the saturation polarization at 300 and 10 K, as a function of Fe concentration. The observed linear dependence would reflect the substitution of Fe by Co moments [7]. We can write:

$$J_S(w) = J_{S,Fe}w + J_{S,Co}(1-w)$$

where $J_{s,Fe}$ and $J_{s,Co}$ are the saturation polarization of the Co-free and Fe-free amorphous alloys, respectively, and w is the atomic fraction Fe/(Fe+Co). Similar results are obtained for $Co_{75-x}Fe_xSi_{15}B_{10}$ amorphous alloys [7]. The average magnetic moment per magnetic atom, $<\mu>$, decreases from 1.8 to 0.7 μ_B as the Fe content decreases (Fig. 1). These values are much lower than those reported for crystalline Fe-Co alloys [8] and amorphous FeCoSiB alloys with lower metalloid concentration (~ 20 at. %) [9]. According to the nearest-neighbor coordination model, the atomic magnetic moment is assumed to depend on the number of magnetic atoms and metalloid atoms in the first nearest-neighbor shell. Therefore, the low value of $<\mu>$ in these amorphous alloys can be attributed to the decrease of the number of the nearest-neighbor magnetic atoms. Similar results are found in $(Fe_{1-x}Co_x)_{62.5}Si_{12.5}B_{25}$ [4], $(Fe_xCo_{100-x})_{73}Si_{17}B_{10}$ and $(Fe_xCo_{100-x})_{76.7}Si_{13.3}B_{10}$ [10] amorphous alloys. The room temperature magnetostriction, λ_S, decreases linearly with Co content from 18×10^{-6} to nearly zero (Fig. 1).

3.2. Influence of annealing technique

Fig. 2 shows the dependence of the coercivity of $Fe_{72-x}Nb_xAl_5Ga_2P_{11}C_6B_4$ (x = 0; 2) for different annealing procedures as a function of the annealing parameters, i.e. annealing temperature, T_A, for FA (20 min duration) and heating power per surface area P_S for CA. We use P_S as CA parameter, which is proportional to the steady state annealing temperature instead of current or current density in order to minimize the errors introduced mainly by the fluctuations of the sample resistance and average sample thickness (for details see [11]). Current annealing was carried out by multi-step heat treatments with successive increases of the heating power.

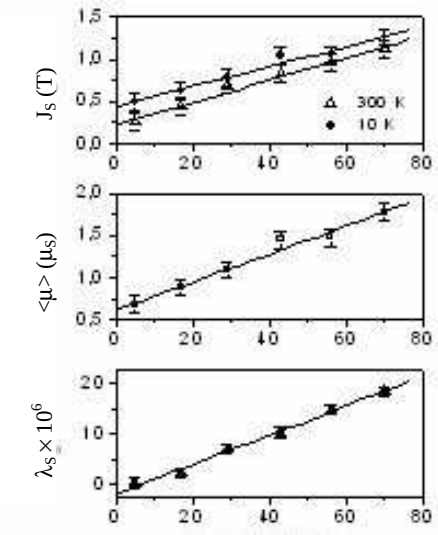

Fig. 1. Saturation magnetization at 300 K and 10 K, magnetic moment per (Fe+Co) atom at 10 K and saturation magnetostriction constant as a function of the Fe content.

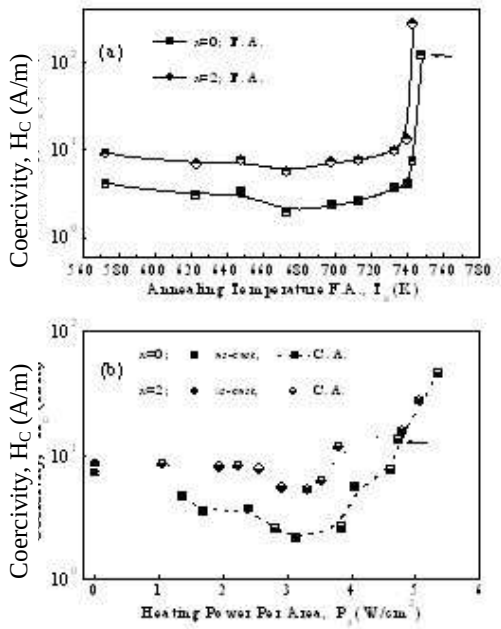

Fig. 2. Coercivity changes in $Fe_{72-x}Nb_x\ Al_5\ Ga_2\ P_{11}C_6B_4$ (x = 0; 2) after different annealing treatments: (a) furnace annealing, (FA), and (b) current annealing; (CA). Arrows indicate coercivity of the samples with similar XRD patterns.

The coercivity shows a minimum as a function of the annealing parameter. The initial decrease of coercivity is due to stress relief whilst the increase towards higher values of T_A or P_S is due to crystallization effects. The lowest coercivities achieved by both annealing methods are similar. However, significant differences in the magnetic hardening are observed between FA and CA crystallized samples.

It can be derived from XRD-peak intensities and TEM micrographs that the crystalline fraction of the CA sample subjected to P_S = 4.73 W/cm^2 is slightly higher than that of the FA sample annealed at 748 K (Fig. 3).

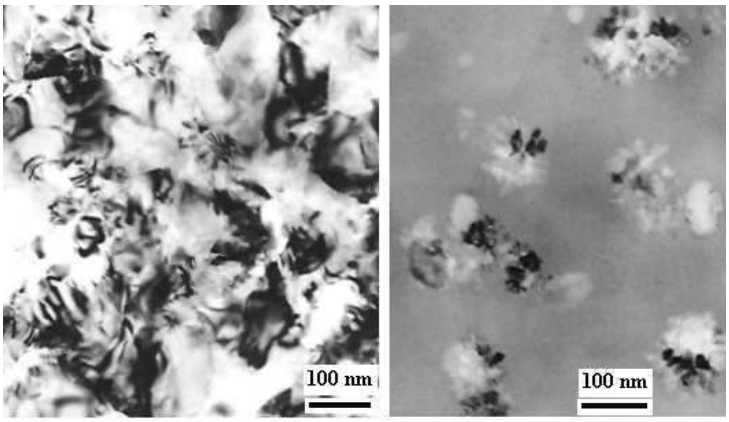

Fig. 3. TEM micrographs of partially crystallized $Fe_{72}Al_5\ Ga_2\ P_{11}C_6B_4$, (a) after CA at 4.73 W/cm^2 and (b) after 20 min at 748 K

But, the coercivity of the CA sample is about one order of magnitude lower than that of the corresponding FA sample. The origin of this behavior is the different crystallization mechanism resulting in different microstructures caused by the high heating and cooling rates assured in the CA technique. The FA sample annealed for 20 min at 748 K is characterized by isolated crystals

embedded in a featureless amorphous matrix, whereas the CA sample after CA at 4.73 W/cm^2 is more uniformly crystallized but with less sharp grain boundaries. Thus, the FA sample appears to be more inhomogeneous, which is the reason for the larger coercivity in spite of the lower fraction of crystallized volume.

3.3. Preparation of bulk samples and comparison with ribbons

Amorphous $Fe_{77}Al_{2,14}Ga_{0,86}P_{8.4}C_5B_4Si_{2.6}$ ribbons and rods were prepared by melt spinning and copper mold casting, respectively. From Table 2 it can be seen that the characteristic temperatures of crystallization and the saturation polarization are equal for both alloys, whilst the Curie temperature and the coercivity are larger for the rod sample. The higher Curie temperature is due to a more relaxed amorphous structure. The larger coercivity may be due to larger internal stresses or to a larger in--homogeneity. Nevertheless, coercivity is small for both types of samples.

Table 2. Magnetic properties and crystallization behaviour of $Fe_{77}Al_{2,14}Ga_{0,86}P_{8.4}C_5B_4Si_{2.6}$ ribbons and rods.

	$T_{C\,am}$, K	λ_s, ppm	J_S, T	H_C, A/m	T_g, K	T_x, K	ΔT_x, K
Ribbon	343	26.5	1.3	4	737	769	32
Rod	352	-	1.3	8÷40	737	769	32

Fig. 4 shows the characteristic times for crystallization as a function of the isothermal annealing temperature, where t_{ons} is the incubation time for crystallization, and t_{infl} is the time at which the evolution of the crystallized volume fraction shows a point of inflection, i.e. where the crystallization rate attains maximum. Crystallization starts earlier and proceeds quicker in the rod sample, which is probably due to pre-formed crystallization nuclei. Thus, the rod sample is characterized by a larger density of nucleation centers. This underlines the importance of nucleation for the process of preparation of bulk amorphous alloys. The presence of an incubation time is distinctive for the fully amorphous samples.

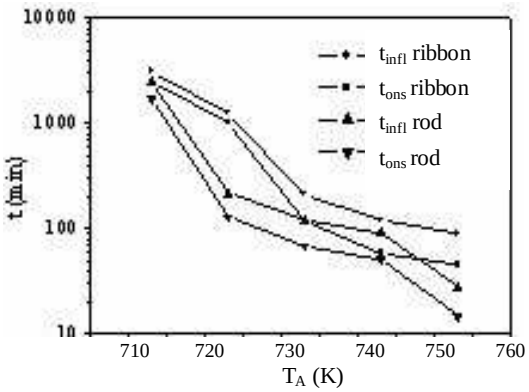

Fig. 4. Characteristic times of crystallization, t, versus isothermic annealing temperature, T_A, for $Fe_{77}Al_{2,14}Ga_{0,86}P_{8.4}C_5B_4Si_{2.6}$ ribbons and rods

Furthermore, bulk amorphous samples were prepared by milling $Fe_{77}Al_{2,14}Ga_{0,86}P_{8.4}C_5B_4Si_{2.6}$ amorphous ribbons and hot pressing the powders in discs-shapes 10 mm in diameter and 4 to 6 mm in height (Fig. 5). Pressing time and pressure were 2 min and 500 MPa, respectively. Fig. 6 shows the dependence of the coercivity on the pressing temperature. After milling, the powder has a coercivity of 2300 A/m. This is due to the severe mechanical damage during high energy ball milling. After hot pressing in the temperature range 720 - 760 K the coercivity drops to values between 100 and 200

A/m. This reduction of the coercivity by more than one order of magnitude is due to the stress relief at elevated temperatures near or above the glass transition temperature. The pressing itself seems not to induce strong stresses considering that the coercivity is rather low after pressing. If the pressing temperature exceeds 760 K the coercivity increases due to the onset of crystallization.

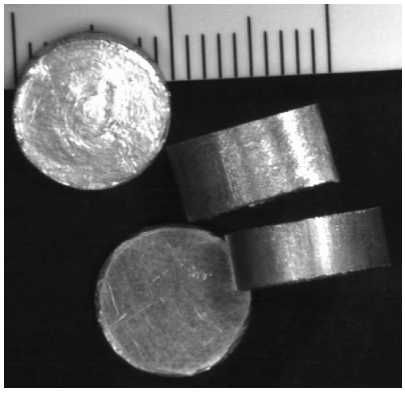

Fig. 5. Hot pressed discs from $Fe_{77}Al_{2,14}Ga_{0,86}P_{8.4}C_5B_4Si_{2.6}$ amorphous alloy powder.

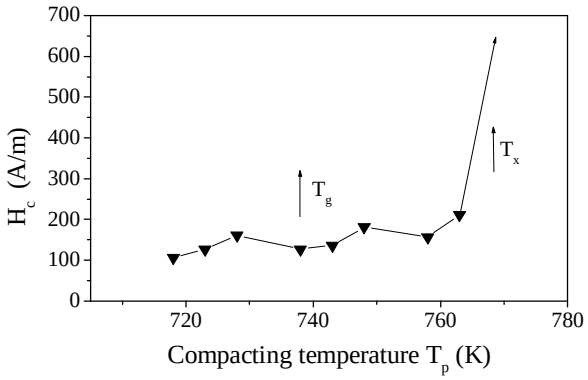

Fig. 6. Influence of the compacting temperature on the coercivity of the ball milled and compacted amorphous $Fe_{77}Al_{2,14}Ga_{0,86}P_{8.4}C_5B_4Si_{2.6}$.

Figs. 7 and 8 show the hysteresis loops of the hot pressed bulk disc, ribbon sample, and rod sample. Coercivity is small for all samples, as already mentioned. The permeability of the powder sample is rather low ($\mu \sim 7$) and constant up to 130 A/cm, whereas both the other samples saturate at fields below 40 A/cm. The different slopes of the hysteresis loops of the rod and the ribbon sample at zero field are due to the different shape anisotropy of these samples.

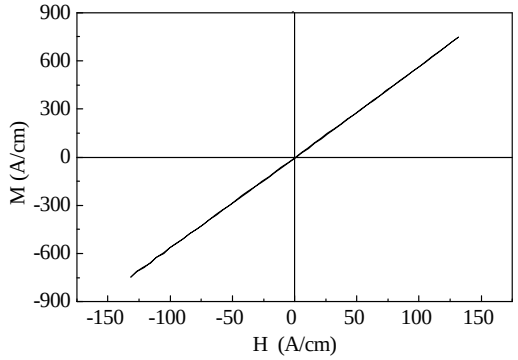

Fig. 7. Field dependence of the magnetization of a hot pressed $Fe_{77}Al_{2,14}Ga_{0,86}P_{8.4}C_5B_4Si_{2.6}$ powder sample, corrected for demagnetizing field.

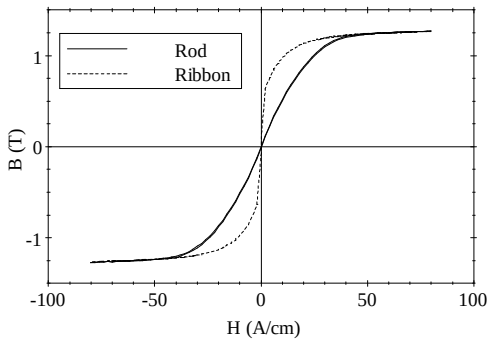

Fig. 8. Field dependence of the magnetic induction of $Fe_{77}Al_{2,14}Ga_{0,86}P_{8.4}C_5B_4Si_{2.6}$ ribbon and rod samples, not corrected for demagnetizing field.

4. Conclusions

Amorphous iron-base alloys with a large supercooled liquid region $\Delta T_x = T_x - T_g$ (where T_x and T_g are the temperatures of glass transition and on-set crystallization, respectively) can be prepared by melt-spinning and copper-mold casting, the latter method allowing to prepare bulk samples. Bulk amorphous samples may also be prepared by high energy milling of amorphous melt-spun ribbons and subsequent hot pressing of the powders to the desired shape. The influence of composition on the intrinsic magnetic properties can be understood within the framework of the theories developed for the description of the intrinsic magnetic properties of metallic glasses, keeping in mind that the metalloids content is larger in these new alloys, and therefore the Curie temperatures and the magnetic

moments are lower. It was shown that the coercivity of these alloys is low as long as crystallization or severe mechanical damage is avoided. Annealing between the glass transition temperature, T_g, and the crystallization temperature, T_x, is effective in reducing internal stresses and coercivity. The type of annealing, conventional furnace annealing or short time current annealing is of minor importance as long as crystallization is avoided.

Acknowledgement

The authors thank N. Mattern and A. Ostwald from IFW Dresden for the XRD measurements and their valuable help on the identification of the crystalline phases and C. Mickel for help and assistance with TEM investigations. This work was partially supported by the European Community in the framework of the EU RTN-Network on bulk metallic glasses (HPRN-CT-2000-0033), by the German Academic Exchange Service (DAAD), by the Saxonian Ministry of Science and Culture, by the DGES of the Spanish Ministry of Education (Project PB97-1119-C02-01), and by the PAI of the Junta de Andalucía.

References

[1] S. Roth, A. R. Ferchmin, S. Kobe; Landolt-Börnstein Series - Numerical Data and Functional Relationships in Science and Technology Vol III/19 - Magnetic Properties of Metals, Ed.: H. P. J. Wijn, Springer - Verlag, Berlin Heidelberg, p. 144, 1994
[2] K. Narita, J. Yamasaki, H. Fukunaga, IEEE Trans. Magn.,**16**, 435 (1980).
[3] M. Müller, H. Grahl, N. Mattern, U. Kühn, B. Schnell, J. Magn. Magn. Mater. **160**, 284 (1996).
[4] B. G. Shen, L. Cao, H. Q. Guo, J. Appl. Phys. **73**, 5730 (1993).
[5] F. E. Luborsky, J. Appl. Phys., **51**, 2808 (1980).
[6] M. L. Fernández-Gubieda, I. Orue, J. M. Barandiarán, F. Plazaola, Non-Crystalline and Nanoscale Materials, Eds. R. Rivas and M.A. López Quintela, World Scientific, Singapore, p. 172, 1997.
[7] M. Knobel, R. Sato Turtelli, R. Grössinger, J. Magn. Magn. Mater. **116**, 154 (1992).
[8] D. I. Bardos, J. Appl. Phys. **40**, 1371 (1969).
[9] M. Goto, H. Tange, T. Tokunaga, Jpn. J. Appl. Phys. **17**, 1877 (1978).
[10] K. Narita, J. Yamasaki, H. Fukunaga, IEEE Trans. Magn. **14**, 1016 (1978).
[11] N. S. Mitrović, S. R. Djukić, S. B. Djurić, IEEE Trans. Magn. **MAG-36**, 3858 (2000).